The Plant Cell, Vol. 19: 2705–2718, September 2007, www.plantcell.org © 2007 American Society of Plant Biologists

RESEARCH ARTICLES

Oryza sativa Dicer-like4 Reveals a Key Role for Small Interfering RNA Silencing in Plant Development [W][OA]

Bin Liu,[a,b] Zhiyu Chen,[a,b] Xianwei Song,[a,b] Chunyan Liu,[a] Xia Cui,[a] Xianfeng Zhao,[a] Jun Fang,[a,b] Wenying Xu,[c] Huiyong Zhang,[d] Xiujie Wang,[a] Chengcai Chu,[a] Xingwang Deng,[d,e] Yongbiao Xue,[c] and Xiaofeng Cao[a,1]

[a] State Key Laboratory of Plant Genomics and National Center for Plant Gene Research, Institute of Genetics and Developmental Biology, Chinese Academy of Sciences, Beijing 100101, China

[b] Graduate University of the Chinese Academy of Sciences, Beijing 100039, China

[c] Laboratory of Molecular and Developmental Biology and National Center for Plant Gene Research, Institute of Genetics and Developmental Biology, Chinese Academy of Sciences, Beijing 100101, China

[d] National Institute of Biological Science, Beijing 102206, China

[e] Department of Molecular, Cellular, and Development Biology, Yale University, New Haven, Connecticut 06520-8104

MicroRNAs and small interfering RNAs (siRNAs) are two classes of small regulatory RNAs derived from different types of precursors and processed by distinct Dicer or Dicer-like (DCL) proteins. During evolution, four *Arabidopsis thaliana* DCLs and six rice (*Oryza sativa*) DCLs (Os DCLs) appear to have acquired specialized functions. The *Arabidopsis* DCLs are well characterized, but those in rice remain largely unstudied. Here, we show that both knockdown and loss of function of rice *DCL4*, the homolog of *Arabidopsis DCL4*, lead to vegetative growth abnormalities and severe developmental defects in spikelet identity. These phenotypic alterations appear to be distinct from those observed in *Arabidopsis dcl4* mutants, which exhibit accelerated vegetative phase change. The difference in phenotype between rice and *Arabidopsis dcl4* mutants suggests that siRNA processing by DCL4 has a broader role in rice development than in *Arabidopsis*. Biochemical and genetic analyses indicate that Os DCL4 is the major Dicer responsible for the 21-nucleotide siRNAs associated with inverted repeat transgenes and for *trans*-acting siRNA (ta-siRNA) from the endogenous *TRANS-ACTING siRNA3* (*TAS3*) gene. We show that the biogenesis mechanism of *TAS3* ta-siRNA is conserved but that putative direct targets of Os DCL4 appear to be differentially regulated between monocots and dicots. Our results reveal a critical role of Os DCL4-mediated ta-siRNA biogenesis in rice development.

INTRODUCTION

MicroRNAs (miRNAs) and small interfering RNAs (siRNAs) are two types of noncoding RNAs that play fundamental roles in developmental regulation, epigenetic modifications, and viral defense (Kidner and Martienssen, 2005; Vaucheret, 2006). miRNAs and siRNAs are very similar in their structural and functional features. Both are 21 to 24 nucleotides in length, with a 5′ phosphate and a 3′ OH, and both serve as sequence-specific regulators to guide target gene repression (Bartel, 2004). However, they are produced from very different types of precursors (Bartel, 2004; Jones-Rhoades et al., 2006). miRNAs originate from single RNA molecules that form imperfect local hairpin-like secondary structures (Lagos-Quintana et al., 2001; Lau et al., 2001; Lee and Ambros, 2001; Reinhart et al., 2002). siRNAs are produced from either endogenous or exogenous long double-stranded RNAs (dsRNAs) with perfect complementarity (Zamore et al., 2000; Elbashir et al., 2001).

Key components in the miRNA and siRNA biogenesis pathways are the Dicer or Dicer-like (DCL) proteins. *Arabidopsis thaliana* encodes four DCL proteins, and the rice (*Oryza sativa*) genome has six putative DCL proteins. Biochemical analysis has shown that Dicer activities producing 21- to 24-nucleotide siRNAs were present in a wheat germ system (Tang et al., 2003). Further biochemical studies also revealed that DCL1 and DCL3 produce 21- and 24-nucleotide siRNAs, respectively, in *Arabidopsis* silencing pathways (Qi et al., 2005). Although molecular and genetic analysis demonstrated that At DCL4 was predominantly involved in the biogenesis of 21-nucleotide *trans*-acting siRNAs (ta-siRNAs), virus-induced siRNAs, and transgenic siRNAs, direct biochemical evidence is lacking (Vazquez et al., 2004; Allen et al., 2005; Gasciolli et al., 2005; Xie et al., 2005; Yoshikawa et al., 2005). Genetic analysis in *Arabidopsis* has revealed both specialized and overlapping functions of Dicer proteins (Fahlgren et al., 2006; Henderson et al., 2006).

DCL1 is required for the maturation of miRNAs, and *dcl1* loss-of-function mutants show pleiotropic developmental defects (Park et al., 2002; Reinhart et al., 2002; Schauer et al., 2002; Kurihara and Watanabe, 2004). All four DCLs appear to be involved in siRNA biogenesis either with specific, redundant or partially compensatory and antagonistic roles reflecting the

[1] Address correspondence to xfcao@genetics.ac.cn.
The author responsible for distribution of materials integral to the findings presented in this article in accordance with the policy described in the Instructions for Authors (www.plantcell.org) is: Xiaofeng Cao (xfcao@genetics.ac.cn).

[W]Online version contains Web-only data.

[OA]Open Access articles can be viewed online without a subscription.

www.plantcell.org/cgi/doi/10.1105/tpc.107.052209

complexity of siRNA production (Xie et al., 2004, 2005; Gasciolli et al., 2005; Yoshikawa et al., 2005; Bouche et al., 2006; Henderson et al., 2006; Margis et al., 2006).

DCL2 is involved in the processing of 22-nucleotide siRNAs derived from *Turnip crinkle virus* (Xie et al., 2004) and 24-nucleotide siRNAs derived from natural antisense transcript pairs under salt stress (Borsani et al., 2005). DCL3 is involved in the biogenesis of 24-nucleotide siRNAs that are derived from endogenous repeated sequences associated with heterochromatin or silenced transgenes (Xie et al., 2004). Neither *dcl2* nor *dcl3* shows developmental defects in *Arabidopsis*.

DCL4 is responsible for the processing of 21-nucleotide ta-siRNAs that are required for normal plant development (Vazquez et al., 2004; Allen et al., 2005; Gasciolli et al., 2005; Xie et al., 2005; Yoshikawa et al., 2005). ta-siRNAs are endogenous and a plant-specific class of siRNAs. The biogenesis of ta-siRNAs requires both DCL1 and DCL4 activities in *Arabidopsis* (Vazquez et al., 2004; Yoshikawa et al., 2005). Transcripts from *TRANS-ACTING siRNA* (*TAS*) genes are cleaved by DCL1-processed miRNAs, and the cleavage products are stabilized by SUPPRESSOR OF GENE SILENCING3 (SGS3) and then amplified by RNA-DEPENDENT RNA POLYMERASE6 (RDR6) to generate dsRNAs that are further processed by DCL4 into ta-siRNAs (Allen et al., 2005; Yoshikawa et al., 2005; Axtell et al., 2006).

Mutations in *DCL4* result in slightly elongated, downward-curled rosette leaves and accelerated juvenile-to-adult vegetative phase change in *Arabidopsis*, suggesting a specific role of the DCL4-mediated ta-siRNA pathway (Gasciolli et al., 2005; Xie et al., 2005; Adenot et al., 2006; Fahlgren et al., 2006). Several *TAS* gene families in *Arabidopsis* have been identified (Vazquez et al., 2004; Rajagopalan et al., 2006; Howell et al., 2007). However, the juvenile-to-adult phase transition is only suppressed by At *TAS3* ta-siRNAs through negative regulation of *Auxin Response Factor3* (*ETT*/*ARF3*) and *ARF4* in *Arabidopsis* (Adenot et al., 2006; Fahlgren et al., 2006; Garcia et al., 2006; Hunter et al., 2006). Moreover, the weak *dcl4* phenotype can be enhanced by overexpression of nontargeted *ARF3* (*ARF3mut*) in the *rdr6* mutant, resulting in further acceleration of phase change and severe developmental defects of leaves and floral organs (Fahlgren et al., 2006).

By contrast with the well-characterized DCL proteins in *Arabidopsis*, little is known about their action in any other plants. Previously, we demonstrated that knockdown of Os *DCL1*, like *Arabidopsis dcl1*, caused pleiotropic phenotypes in rice due to a failure of miRNA metabolism (Schauer et al., 2002; Liu et al., 2005). However, phylogenetic analysis suggested that the functional diversification of DCLs occurred before the divergence of monocots and dicots ~200 million years ago (Henderson et al., 2006; Margis et al., 2006). Therefore, it is possible that during evolution, rice and *Arabidopsis* DCLs might have acquired distinct functions in small RNA biogenesis and/or plant development for each species.

Here, we analyze the role of DCL4 in rice and compare it with that of DCL4 in *Arabidopsis*. Biochemical and genetic analyses demonstrate that Os DCL4 generates 21-nucleotide siRNAs in vitro and is responsible for 21-nucleotide siRNA production derived from inverted repeat transgenes and *TAS3* ta-siRNA biogenesis, indicating the fundamental similarity of the ta-siRNA pathways between rice and *Arabidopsis*. By contrast, loss of function of Os DCL4 leads to vegetative developmental defects and severe disruption of spikelet organ identity, resulting in sterility, revealing a much broader role for Os DCL4 in development than for its *Arabidopsis* counterpart. Furthermore, we identify an endogenous mRNA with a long fold-back structure that could be processed by Os DCL4 into 21-nucleotide siRNAs, supporting the hypothesis that miRNA genes are evolved from inverted duplication of target genes (Allen et al., 2004), thus providing further evidence for an evolutionary link between siRNA and miRNA.

RESULTS

Knockdown of Os *DCL4* Results in Abnormal Spikelet Morphology

In other organisms, RNA interference (RNAi) has been used successfully to study the components involved in the RNAi pathway (Dudley et al., 2002; Kim et al., 2005). To determine the role of Os DCL4 encoded by Os *04g43050* in small RNA biogenesis and rice development, 15 individual transgenic plants expressing an inverted repeat of Os *DCL4* (*DCL4IR*) were generated (Liu et al., 2005). During reproductive development, the basic branching architecture of the panicle in *DCL4IR* transformants was normal except for the absence of certain spikelets in the lower part of the rachis (Figures 1A and 1B). A spikelet, the basic morphological unit of the rice inflorescence, contains a pair of empty glumes and a pair of bract-like structures named the lemma and the palea, which function like sepals of other plants (Schmidt and Ambrose, 1998; Ferrario et al., 2004; Prasad et al., 2005) (Figure 1C). Compared with wild-type plants (Figure 1C), spikelet organ identity was greatly disrupted in the *DCL4IR* transformants (Figures 1D to 1F). Three typical phenotypes from weak to strong were observed, including a slight opening between the lemma and the palea (Figure 1D) and the lemma being partially or completely degenerated to the awn (Figures 1E and 1F). Moreover, the empty glumes and the rudimentary glumes were separated in *DCL4IR* transformants (Figures 1D to 1F) instead of being close together, as in the wild-type control (Figure 1C). As a result, the strong loss-of-function transgenic plants (Figure 1F) were sterile and only two weak loss-of-function plants could produce seeds for further genetic analysis (Figure 1D). The offspring from the weak loss-of-function plants (Figure 1D) showed the expected 1:3 segregation of normal to abnormal phenotype. When 41 T1 plants from two individual transgenic lines were examined, the abnormal phenotype cosegregated with the *DCL4IR* transgenes (Figure 1G). Previously, we showed that Os *DCL4* mRNA levels were reduced but those of the other *DCLs* were not in *DCL4IR* transformants (Liu et al., 2005). Therefore, we conclude that the significant reduction or loss of function of Os *DCL4* caused abnormal spikelet morphology in rice and that the phenotypic variations could be due to variable RNAi efficiency within individual spikelets.

Identification of an Os *dcl4* Recessive Mutant

By searching for mutants with similar phenotypes to the strong *DCL4IR* loss-of-function transformants, we isolated a natural

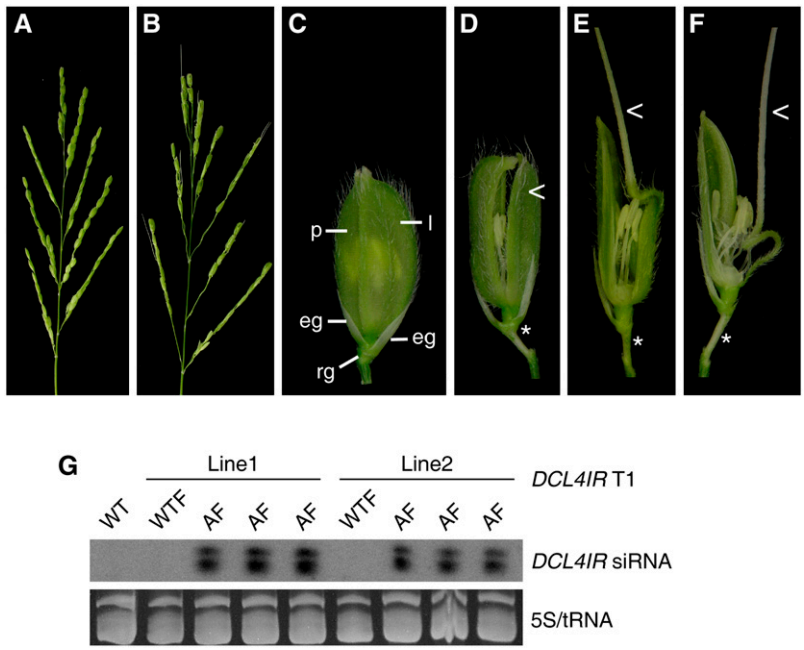

Figure 1. Knockdown of Os *DCL4* Causes Abnormal Morphology in Rice.

(A) An inflorescence of wild-type Nipponbare rice.
(B) An inflorescence of *DCL4IR* transgenic rice.
(C) A spikelet of wild-type rice. The palea (p), lemma (l), a pair of empty glumes (eg), and a pair of rudimentary glumes (rg) are indicated.
(D) to **(F)** The spikelets of *DCL4IR* transformants showing weak **(D)**, intermediate **(E)**, and strong **(F)** phenotypes. Asterisks represent the space between the empty glume and the rudimentary glume; carets indicate the impaired lemma.
(G) Small RNA gel blot analysis of *DCL4IR* siRNA levels (indicated at right) in wild-type and *DCL4IR* transgenic progeny (WTF and AF, respectively). Line 1 and line 2 are two independent T1 generation lines of *DCL4IR* transformants. AF, transgenic plants displaying abnormal flowering; WTF, wild-type phenotypic progeny. 5S/tRNA stained with ethidium bromide was used as a control.

mutant from rice strain L16S of the *indica* variety background (Figure 2A). In this mutant, full-length *DCL4* mRNA was not detectable by RT-PCR (Figure 2B). Sequence analysis showed that *DCL4* mRNA is composed of 26 exons and encodes a polypeptide with 1657 amino acids (Figures 2C and 2D). DNA sequencing of Os *DCL4* from the natural mutant revealed a 1428-bp deletion corresponding to the promoter, the 5′ untranslated region, and the leading 72 bp in the first exon of the gene (Figure 2D). We thus named the natural mutant *dcl4-1*.

To confirm that the abnormal spikelet phenotype in *dcl4-1* was caused by loss of function of Os *DCL4*, we introgressed *dcl4-1* into *indica* variety 9311 with two backcrosses. The F1 plants displayed a normal phenotype, and in the F2 progeny, segregation at a ratio of ~1:3 (660:2175) between mutant and wild-type plants was observed. The abnormal phenotypes cosegregated with *dcl4-1* homozygotes when 660 F2 plants were examined, indicating that the lesion causing abnormal spikelet phenotypes was tightly linked to the Os *DCL4* locus.

Os *dcl4* Mutants Undergo Abnormal Juvenile and Adult Vegetative Development

Vegetative development in rice consists of three stages: juvenile (one to two leaves), intermediate (three to five leaves), and adult (six leaves to flowering) (Itoh et al., 2005). The transitions between these stages are gradual (Asai et al., 2002). During the juvenile stage, *dcl4-1* mutants displayed abnormal coleoptiles and leaf phenotypes compared with wild-type plants (Figure 2E). In the wild type, the first two leaves were rolled up inside the coleoptile or the first leaf sheath to form a cone (Figure 2E, left panel). However, *dcl4-1* mutants produced radialized coleoptiles, and the first and second leaves were not enclosed by the coleoptile or the first leaf, respectively (Figure 2E, right panel, top). With lower (5 to 10%) frequency, severe phenotypes were observed, including development of the first leaf into a thread-like structure (Figure 2E, right panel, bottom). By the intermediate stage, nearly normal leaf phenotypes of *dcl4-1* plants were observed, except that leaves were shorter than those of the wild type (Figure 2F). In the mature stage, *dcl4-1* mutant plants appeared semidwarfed in stature (see Supplemental Figure 1 online).

For further anatomical analyses of the coleoptiles and the first leaf sheaths, we made transverse sections of the wild type and *dcl4-1* at 3.5 d after germination (DAG). In the wild type, the coleoptile formed a circle with the two vascular bundles opposite each other on either side (Figure 2G, left panel). In addition, wild-type coleoptiles displayed adaxial/abaxial polarization, with ~10 layers of differentiated mesophyll cells between the adaxial and

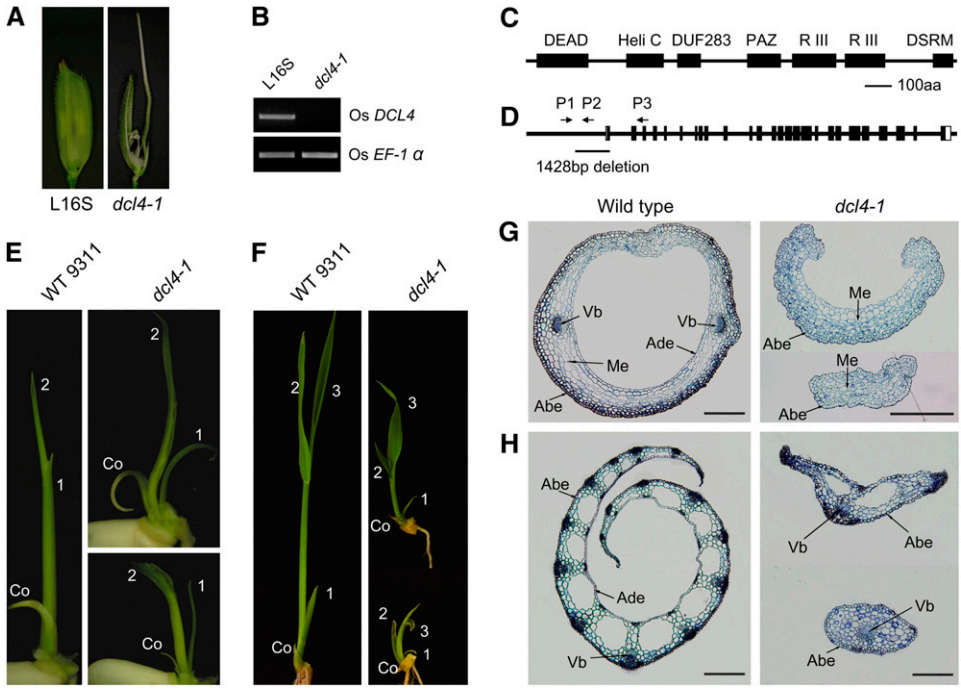

Figure 2. Identification of a Loss-of-Function *dcl4* Mutant.

(A) The spikelet phenotype of *dcl4-1* (right) and its parent L16S (left).
(B) RT-PCR analysis of Os *DCL4* expression levels in wild-type L16S and *dcl4-1*. Os *EF-1*α was used as an internal control.
(C) The domain structure of Os DCL4 protein. Conserved domains are shown as black boxes. DEAD, DEAD box helicase; Heli C, helicase conserved C-terminal domain; DUF283, domain of unknown function 283; PAZ, the PAZ domain, which is named after the proteins Piwi, Argonaut, and Zwille; R III, ribonuclease III domain; DSRM, dsRNA binding motif. Bar = 100 amino acids (aa).
(D) Schematic representation of the Os *DCL4* gene and the location of the *dcl4-1*mutation. Exons are shown as black boxes and introns are shown as lines. The 3′ untranslated region is shown as an open box. The black bar indicates the 1428-bp deletion in the promoter and the 72-bp deletion in the first exon of Os *DCL4* in *dcl4-1*. P1, forward primer; P2, reverse primer located within the deletion region; P3, reverse primer. Primers are used for genotyping of the *dcl4-1*mutation.
(E) and **(F)** Phenotypes of *dcl4-1* in the juvenile vegetative stage. Seedlings of the wild type (left panels) and *dcl4-1* (right panels) at 3.5 DAG **(E)** and 8 DAG **(F)**. Co, coleoptile; 1 to 3, first, second, and third leaves.
(G) and **(H)** Anatomy of wild-type and *dcl4-1* coleoptiles **(G)** and first leaf sheaths **(H)** at 3.5 DAG. In the right panels of *dcl4-1*, the top and bottom plants represent the majority and some thread-like leaves of *dcl4-1* plants, respectively. Abe, abaxial epidermis; Ade, adaxial epidermis; Me, mesophyll; Vb, vascular bundle. Bars = 200 μm.

abaxial epidermises (Figure 2G, left panel). In contrast with the coleoptiles of wild-type plants, the coleoptiles of *dcl4-1* plants lacked the two vascular bundles (Figure 2G, right panel, top). In addition, the shapes of the sheath and margins of the mature first leaves were different between the wild type and *dcl4-1*. In the wild type, the sheath is fully developed with multiple vascular bundles, and the margin of the sheath is pointed and membranous (Itoh et al., 2005). The first leaves of *dcl4-1* mutants displayed a reduced number of vascular bundles and abnormally thick margins (Figure 2H, right panel, top). In some severe *dcl4-1* mutants, single vascular bundles were observed from thread-like leaves (Figure 2H, right panel, bottom).

Moreover, transverse sectioning analysis also revealed the adaxial/abaxial polarity alteration in both coleoptiles and the first leaves in *dcl4-1* (Figures 2G and 2H). In wild-type coleoptiles, abaxial and adaxial surfaces had distinct epidermal cells. The abaxial epidermal cells were relatively small and arranged densely, whereas the adaxial epidermal cells were rectangular in shape and arranged into a smooth surface (Figure 2G, left panel). By contrast, the adaxial epidermis of *dcl4-1* developed into an irregular shape (Figure 2G, right panel, top), and part of the adaxial epidermis displayed abaxial characteristics, especially in those severe mutants (Figure 2G, right panel, bottom). In addition, typical adaxial epidermal cells of the first leaves are present in the wild type; however, the adaxial epidermis of *dcl4-1* mutants partial or fully transformed into densely arranged abaxial epidermis (Figure 2H, right panel). These observations indicate that Os *DCL4* plays an important role in the adaxial/abaxial polarization of the coleoptiles and the first leaves.

Lemma Polarity Is Disrupted in Os *dcl4* Mutants

In the reproductive stage, the lemma and palea of the rice *DCL4IR* transformants and *dcl4-1* mutants showed severe abnormalities. We determined the stage of onset of these abnormalities using scanning electron microscopy (Itoh et al., 2005)

(Figure 3). We did not observe clear developmental differences between *DCL4IR* transformants and wild-type plants during stages Sp1 to Sp6 (Figures 3A to 3F; data not shown). The lemma of *DCL4IR* transformants elongated ectopically during Sp7 (the stage at which the carpel forms and stamens differentiate into filaments and anthers) (Figures 3G and 3H). During Sp8, the apical part of the lemma in the *DCL4IR* transformants tended to become a needle-like awn and the inner reproductive organs were not enclosed by the lemma and palea as they were in wild-type plants (Figures 3I and 3J).

During the heading stage, the wild-type lemma showed shaggy abaxial (Figure 3K) and smooth adaxial (Figure 3L) epidermis. By contrast, the lemma of *dcl4-1* developed into a radial abaxialized awn (Figure 3M, left panel), with the whole epidermis displaying abaxial characteristics (Figure 3M, right panel). This observation indicated that the polarity of the lemma was completely disrupted in *dcl4-1*.

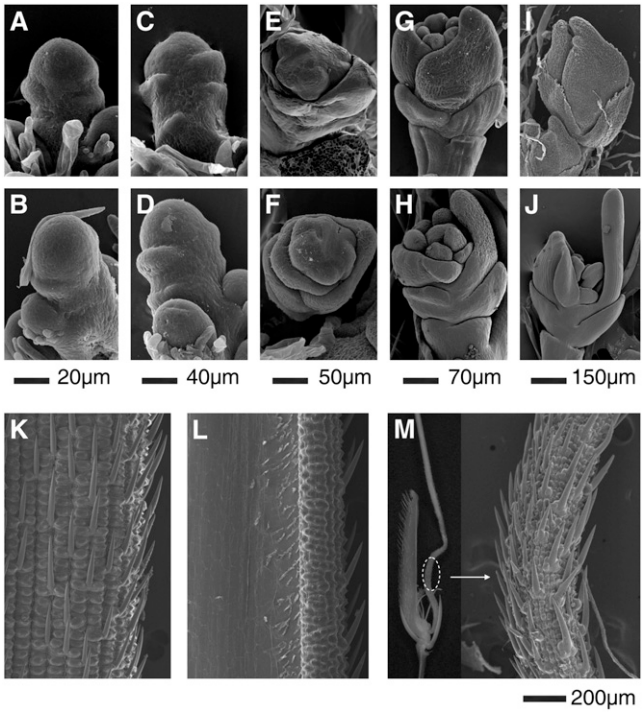

Figure 3. Scanning Electron Microscopy Images of Spikelet Organs.

(A) to **(J)** Top panels, wild-type Nipponbare; bottom panels, *DCL4IR* transformants.

(A) and **(B)** Stage Sp1 to Sp2, formation of a pair of primordia of rudimentary glume and empty glume, respectively.

(C) and **(D)** Stage Sp2 to Sp3, formation of lemma primordium.

(E) and **(F)** Stage Sp5 to Sp6, formation of lodicule and stamen primordia, respectively.

G) and **(H)** Stage Sp7, formation of carpel primordium.

(I) and **(J)** Stage Sp8, ovule and pollen formation.

(K) Scanning electron microscopy image of wild-type 9311 lemma abaxial epidermis.

(L) Scanning electron microscopy image of wild-type 9311 lemma adaxial epidermis.

(M) A spikelet of *dcl4-1* (left panel) and scanning electron microscopy image of its lemma epidermis (right panel).

Scale bars are shown below each stage.

Os DCL4 Provides the Main Dicer Activity for Generating 21-Nucleotide siRNAs

The unique phenotype of the *dcl4-1*mutant prompted us to analyze the role of Os DCL4 in small RNA biogenesis. Previously, we showed that knockdown of Os *DCL4* in *DCL4IR* plants did not affect miRNA biogenesis (Liu et al., 2005). This result was confirmed by analysis of rice carrying the *dcl4-1* null allele. Therefore, the abnormal phenotype is not due to defects in miRNA accumulation (see Supplemental Figure 2 online). Because direct biochemical evidence for DCL4 protein activity in plants is lacking, we performed a biochemical analysis for DCL4 activity in rice. Using protein extracts from young flowers or 30-d-old callus as enzyme sources and the dsRNA of the β-*glucuronidase* (*GUS*) gene as substrate, both 21- and 24-nucleotide siRNAs could be detected when hybridized with sense (Figure 4A, top panel) and antisense (Figure 4A, bottom panel) RNA probes, indicating that Dicer-like activities generating 21- and 24-nucleotide siRNAs exist in both rice tissues tested. By comparing the Dicer-like activities in the extracts from young flower tissues of wild-type and *dcl4-1* plants, we found that extract from *dcl4-1* could produce 24-nucleotide siRNAs with reduced 21-nucleotide siRNAs (Figure 4B). This result provides direct biochemical evidence that efficient 21-nucleotide siRNA production in rice requires *DCL4*.

Os DCL4 Is Required for the Production of 21-Nucleotide siRNAs

It is well established that overexpression of an inverted repeat often leads to transgene silencing associated with the production of 21-, 22-, and 24-nucleotide siRNAs (Mette et al., 2000). To examine the specific role of Os DCL4 in siRNA biogenesis, we studied small RNAs corresponding to the inverted repeat region of the Os *DCL4IR* transgene (Figure 5A, top, left panel). The 22- and 24-nucleotide siRNAs, but not the 21-nucleotide siRNAs, were easily detected in the *DCL4IR* transformants (Figure 5B, left panel). To determine whether the absence of 21-nucleotide siRNAs in the *DCL4IR* transformants is a general phenotype, a transgenic line containing an inverted repeat of the *PHYTOCHROMOBILIN SYNTHASE* (*PSIR*) gene was crossed into *DCL4IR* transformants (Figure 5A). The resulting F1 plants containing both *DCL4IR* and *PSIR* transgenes were examined. siRNAs derived from the *PSIR* inverted repeat with lengths of 21, 22, and 24 nucleotides were all detected in the *PSIR* lines (Figure 5B, middle panel). The 21-nucleotide *PSIR* siRNAs, but not the 22- and 24-nucleotide *PSIR* siRNAs, were almost eliminated in the *PSIR* lines carrying *DCL4IR* (Figure 5B, right panel). We conclude that the production of the 21-nucleotide siRNAs in rice requires Os DCL4 function (Figure 5).

Conserved Biogenesis Mechanism of *TAS3* ta-siRNAs between Monocots and Eudicots

In pursuing the candidate target genes downstream of Os DCL4, we took a whole genome approach to compare transcript profiles in the young inflorescences of wild-type Nipponbare and *DCL4IR*

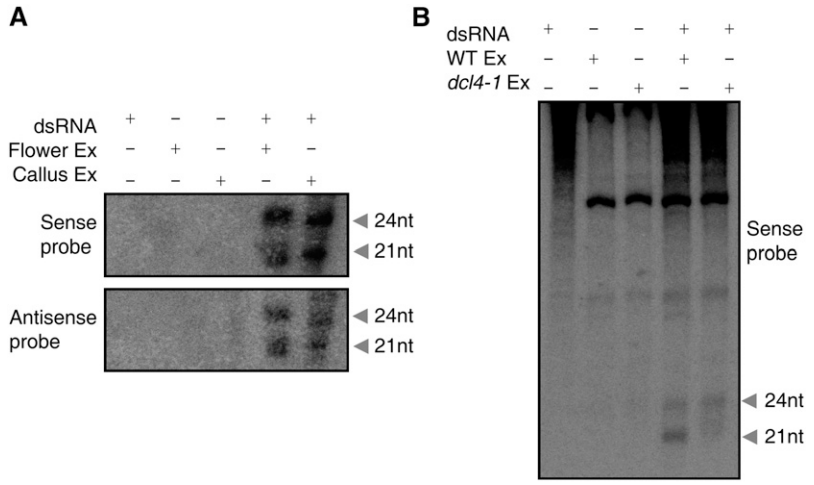

Figure 4. Dicer-Like Activity Assay in Rice.

(A) A 568-bp dsRNA, flower extract (Flower Ex), or callus extract (Callus Ex) were mixed as shown at top. The siRNAs originating from dsRNA of the *GUS* gene were detected using the sense strand (top panel) or the antisense strand (bottom panel) as a probe. nt, nucleotides.

(B) The dsRNA was incubated with wild-type or *dcl4-1* extract as shown at top. siRNAs were detected by sense strand ^{32}P-labeled RNA probe. The positions of the produced 21- and 24-nucleotide siRNAs are indicated.

transformants (Ma et al., 2005) (see Supplemental Table 1 online). An *Auxin Response Factor* gene from rice (Os *ARF*, Os *01g48060*) showed upregulation in the *DCL4IR* transformants. The closest homologous gene, *ARF3* in *Arabidopsis*, is a direct target of *TAS3* ta-siRNAs (Allen et al., 2005; Adenot et al., 2006; Fahlgren et al., 2006; Garcia et al., 2006; Hunter et al., 2006). Phylogenetic analysis indicated that *TAS3* is conserved between *Arabidopsis* and rice (Allen et al., 2005; Williams et al., 2005). In order to test whether Os *DCL4* plays a role in ta-siRNA biogenesis in rice, we first analyzed the sequences of Os *TAS3* (CI412792) to confirm that Os *TAS3* ta-siRNAs exist in rice (Figure 6A). By comparing consecutive 21-nucleotide-long sequences 5′ to the miR390 directed cleavage point, we were able to identify two pairs of highly homologous 21-nucleotide-long sequences between *Arabidopsis* and rice, the At *TAS3* 5′D7(+) versus the Os *TAS3* 5′D6(+) and the At *TAS3* 5′D8(+) versus the Os *TAS3* 5′D7(+), which indicated that Os *TAS3* 5′D6(+) and 5′D7(+) are bona fide ta-siRNAs (Figures 6A and 6B) (Allen et al., 2005).

To determine whether any DCLs play a role in ta-siRNA biogenesis in rice, we compared the expression levels of Os *TAS3* ta-siRNAs between *DCL1IR* and *DCL4IR* transformants and wild-type Nipponbare controls. Levels of Os *TAS3* 5′D6(+) ta-siRNAs were substantially reduced in both the *DCL1IR* and *DCL4IR* transformants (Figure 6C, left panel). Consistent with impaired Os *TAS3* 5′D6(+) ta-siRNA biogenesis in the *DCL4IR* transformants, *dcl4-1* also displayed decreased expression of Os *TAS3* ta-siRNAs (Figure 6C, right panel), indicating that the Os DCL4 activity is required for the biogenesis of ta-siRNAs in rice and that the ta-siRNA biogenesis mechanism is conserved between monocots and eudicots.

Os DCL4 Regulates Multiple Os *ARF* Genes

Computational and experimental methods have identified and validated *ARF2*, *ARF3*, and *ARF4* as targets of *TAS3* ta-siRNA regulation in *Arabidopsis* (Allen et al., 2005; Williams et al., 2005). Sequence comparison analysis identified four close homologs of *Arabidopsis ARF3* and one homolog of *Arabidopsis ARF2* in rice (Williams et al., 2005) (Figure 7A). Among these, the four *ARF3* homologs contained two putative target sites for both Os *TAS3* 5′D6(+) and Os *TAS3* 5′D7(+) ta-siRNAs (Figure 7B, Os *01g48060* as an example), while the *ARF2* homolog (Os *01g70270*) had only one target site for Os *TAS3* 5′D6(+) and Os *TAS3* 5′D7(+) ta-siRNAs.

Transcript levels of the five Os *ARF* genes in *dcl4-1* and wild-type 9311 were compared at 6 DAG and at inflorescence stage 7 (the floral organ differentiation stage) (Itoh et al., 2005). The expression level of Os *01g54990* was upregulated by about fourfold in seedlings and inflorescences of *dcl4-1*(Figure 7C, left panel). The transcripts of Os *05g43920*, Os *01g48060*, and Os *05g48870* were upregulated by about twofold in seedlings and inflorescences of *dcl4-1* (Figure 7C, middle three panels). The expression of the *Arabidopsis ARF2* homolog Os *01g70270* was not changed significantly (Figure 7C, right panel). The differences in expression between individual Os *ARF* genes regulated by Os *TAS3* ta-siRNAs may be related to the developmental regulation of Os DCL4 function.

Endogenous 21-Nucleotide siRNAs Derived from an Imperfect Inverted Repeat of *AK120922* Are Processed by Os DCL4

In our microarray analysis, a unique transcript (*AK120922*) (Kikuchi et al., 2003) showed threefold higher expression in *DCL4IR* transformants compared with that of the wild type. *AK120922* is a rice-specific sequence that has no conserved homolog in currently available genome sequences of any other species. The transcript of *AK120922* can form a hairpin-like structure with a number of mismatches, which is structurally similar to known

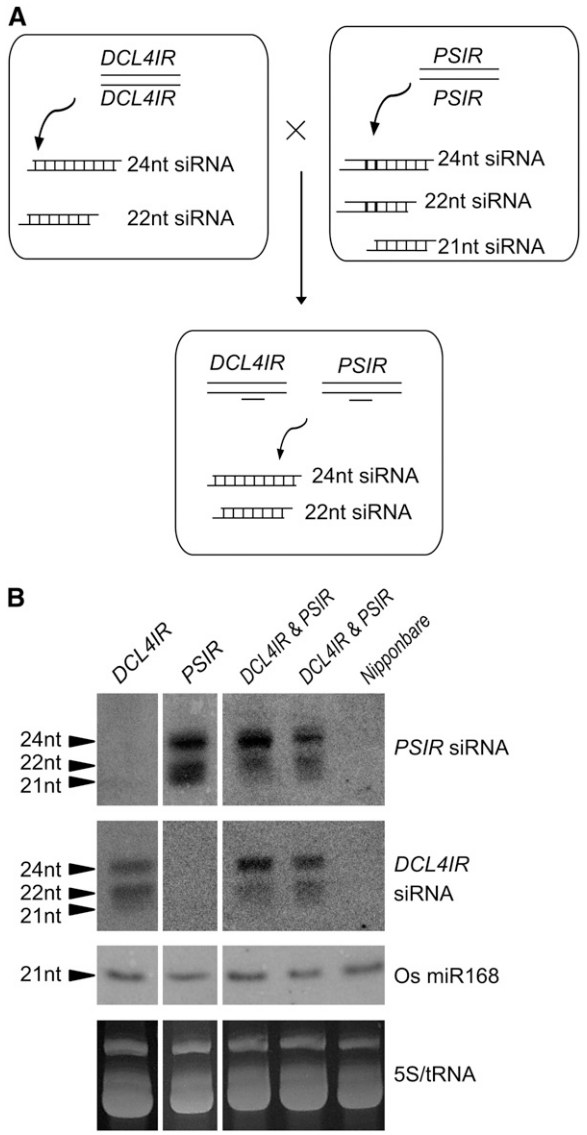

Figure 5. Os DCL4 Acts in the Biogenesis of 21-Nucleotide siRNAs Associated with the Transgene.

(A) Diagrammatic representation of the biogenesis of 21-, 22-, and 24-nucleotide (nt) siRNAs in *DCL4IR* transformants, *PSIR* transformants, and their crossed offspring.

(B) Small RNA gel blot analysis of inverted repeat–associated siRNAs. Samples from *DCL4IR* transformants (*DCL4IR*), *PSIR* transformants (*PSIR*), and two double mutants (*DCL4IR* and *PSIR*) are listed at top. The wild type (Nipponbare) was used as a negative control. Os miR168 and 5S/tRNA stained with ethidium bromide were used as loading controls (bottom two panels).

miRNA precursors or putative transitional RNA genes (containing a long fold-back structure with very few mismatches) (Figure 8A) (Allen et al., 2004).

To confirm that the increased transcript levels of *AK120922* resulted from loss of function of Os *DCL4*, RNA gel blot analysis was performed using a probe corresponding to the entire top arm of the inverted repeat region of *AK120922* (Figures 8A and 8B). As expected, the level of the full-length *AK120922* was increased in *DCL4IR* and *dcl4-1* plants compared with the wild-type controls, indicating that *AK120922* was indeed processed by Os DCL4 in wild-type plants.

As shown in Figure 8A, 21- and 22-nucleotide small RNAs that have been cloned previously and identified as Os miR436 (Sunkar et al., 2005a) and P7-E5 siRNA (Sunkar et al., 2005b), respectively, may originate from the *AK120922* fold-back region. Data from the small RNA Massively Parallel Signature Sequencing database (http://mpss.udel.edu/rice/) revealed that large amounts of small RNAs were generated from the *AK120922* transcript (see Supplemental Figure 4 online) (Nobuta et al., 2007). In order to determine whether the small RNAs derived from *AK120922* were miRNAs or siRNAs, small RNA gel blots were used to examine their accumulation in *DCL1IR* and *DCL4IR* transformants and in the *dcl4-1* mutant (Figure 8C). We found that expression of 21-nucleotide small RNAs corresponding to the top arm of the inverted repeat region was eliminated in *DCL4IR* transformants and *dcl4-1* but not in the wild-type Nipponbare, the *DCL1IR* transformants, or the L16S rice strain (the wild-type control for *dcl4-1*). Similar results were also obtained when a different probe for that region was used (the top arm of the inverted repeat region that does not overlap the Os miR346 region). Interestingly, when a more sensitive lock-modified DNA (LNA) probe corresponding to the small RNA of Os miR436 was used, 21-nucleotide siRNAs appeared to be reduced in *DCL4IR* and *dcl4*, while the levels of 22- and 24-nucleotide siRNAs were not changed (Figure 8C). This result demonstrates the specificity of Os DCL4 in the production of 21- but not 22- or 24-nucleotide siRNAs. By contrast, the expression level of Os miR168 was reduced in *DCL1IR* but not *DCL4IR* transformants. Our results suggest that the small RNAs derived from *AK120922*, including the previously reported Os miR436, are siRNAs, unless they are redefined as special miRNAs produced by Os DCL4 (Rajagopalan et al., 2006).

DISCUSSION

The role of RNA silencing in plant development has been the focus of much recent research activity. miRNAs generated by DCL1 are known to regulate the expression of numerous key developmental genes (Jones-Rhoades et al., 2006). Our previous work indicates that Os *DCL1* is exclusively responsible for miRNA biogenesis, and lesions in Os *DCL1* cause pleiotropic developmental defects similar to *Arabidopsis dcl1* mutants (Liu et al., 2005). ta-siRNAs processed by DCL1 and DCL4 activities are involved in leaf development in *Arabidopsis*. This study describes the role of Os DCL4 in rice, showing its biochemical functions to be conserved with *Arabidopsis*, but with a much broader role in developmental regulation.

Os DCL4 Loss-of-Function Rice Mutants Display Phenotypes Distinct from Their *Arabidopsis* Counterparts

Here, we demonstrate that Os DCL4 is the main, if not sole, enzyme that generates 21-nucleotide siRNAs in vivo. We also prove that Os DCL4 is responsible for the production of the

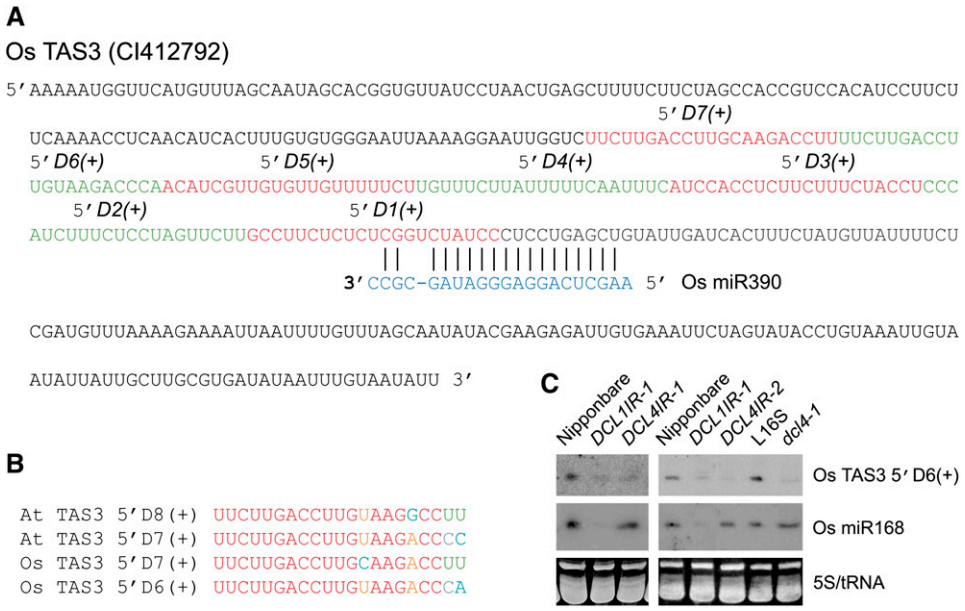

Figure 6. Characterization of the Biogenesis and Function of Os *TAS3* ta-siRNAs.

(A) The diagram represents the biogenesis of predicted Os *TAS3* ta-siRNAs from Os *TAS3* transcript directed by Os miR390 (blue). Putative ta-siRNAs are shown alternately in red and green.

(B) Alignment of At *TAS3* ta-siRNAs and Os *TAS3* ta-siRNAs. Os *TAS3* 5′D6(+) is homologous with At *TAS3* 5′D7(+), and Os *TAS3* 5′D7(+) is homologous with At *TAS3* 5′D8(+).

(C) Accumulation of Os *TAS3* ta-siRNAs in *DCL1IR*, *DCL4IR* transformants, and *dcl4-1* as revealed by RNA gel blot analysis. Nipponbare was used as a control for *DCL1IR* and *DCL4IR* transformants; L16S was the wild-type control for *dcl4-1*. Os miR168 and 5S/tRNA stained with ethidium bromide were used as loading controls in the middle and bottom panels, respectively.

21-nucleotide siRNAs derived from inverted repeat transgenes and endogenous ta-siRNAs. Although the ta-siRNA biogenesis mechanism is conserved between monocots and eudicots, rice *DCL4IR* transformants and *dcl4-1* mutants display severe lateral organ polarity defects in contrast with *Arabidopsis dcl4* mutants.

In *Arabidopsis*, *dcl4* mutants display inconspicuous leaf changes, including downward-curled rosette leaves and increased ratio of length to width, as well as accelerated juvenile-to-adult vegetative phase changes indicated by the appearance of trichomes on the abaxial epidermis in leaves (Gasciolli et al., 2005; Xie et al., 2005; Yoshikawa et al., 2005; Adenot et al., 2006; Fahlgren et al., 2006). By contrast, the rice *dcl4-1* mutants display abnormal coleoptiles in which the two vascular bundles are undeveloped. Furthermore, the first leaves of *dcl4-1* plants have a reduced number of vascular bundles and abnormally thick margins and even form thread-like leaves with abaxialized epidermis and single vascular bundles (Figure 2H). These phenotypes of *dcl4-1* resemble phenotypes caused by the ectopic expression of *KANADI*, a member of the GARP-type transcription factor in *Arabidopsis*, which results in abaxialized cotyledons and inhibits the formation of vascular bundles (Eshed et al., 2001; Kerstetter et al., 2001). In the reproductive stage, the lemmas of *dcl4-1* mutants develop into awn-like organs with abaxialized epidermis and spikelet organ identity is disrupted, resulting in sterility. While other regulatory pathways, in addition to that including TAS3, may be involved in regulating leaf polarity, the extent to which the different pathways are used may vary between different organs. The most obvious defects of lemma in *dcl4-1* indicate that the TAS3-containing pathway plays a critical role in the determination of lemma polarity. Recently, Nagasaki et al. (2007) have independently reported that the Os DCL4 (also known as SHOOT ORGANIZATION1)–mediated ta-siRNA pathway regulates the critical step of shoot apical meristem formation during rice embryogenesis. In conclusion, loss-of-function mutations of Os DCL4 cause severe developmental defects in rice but not in *Arabidopsis*. The striking phenotypes of *dcl4-1* rice mutants indicate the essential role of Os DCL4 in siRNA biogenesis for rice development, especially for normal lateral organ polarity.

Involvement of the siRNA Pathway in Leaf Polarity Control in Different Plant Species

In *Arabidopsis*, the protein-coding genes *ASYMMETRIC LEAVES1* (*AS1*) and *AS2* and the ta-siRNA–encoding *TAS3* gene redundantly regulate leaf polarity (Garcia et al., 2006; Kidner and Timmermans, 2007). Mutations in neither *TAS3* nor *AS1* show obvious defects. Only double mutants between *as1* and the ta-siRNA pathway show enhanced leaf-patterning defects (Garcia et al., 2006). Here, we demonstrate that *dcl4* single mutants develop severe lateral organ polarity defects, implying that the ta-siRNA pathway plays a critical role in the development of adaxial/abaxial leaf polarity in rice. Similarly, *leafbladeless* (*lbl1*) is the maize (*Zea mays*) homolog of *Arabidopsis SGS3*, and severe *lbl1* mutants also develop radially symmetric, thread-like leaves and exhibit

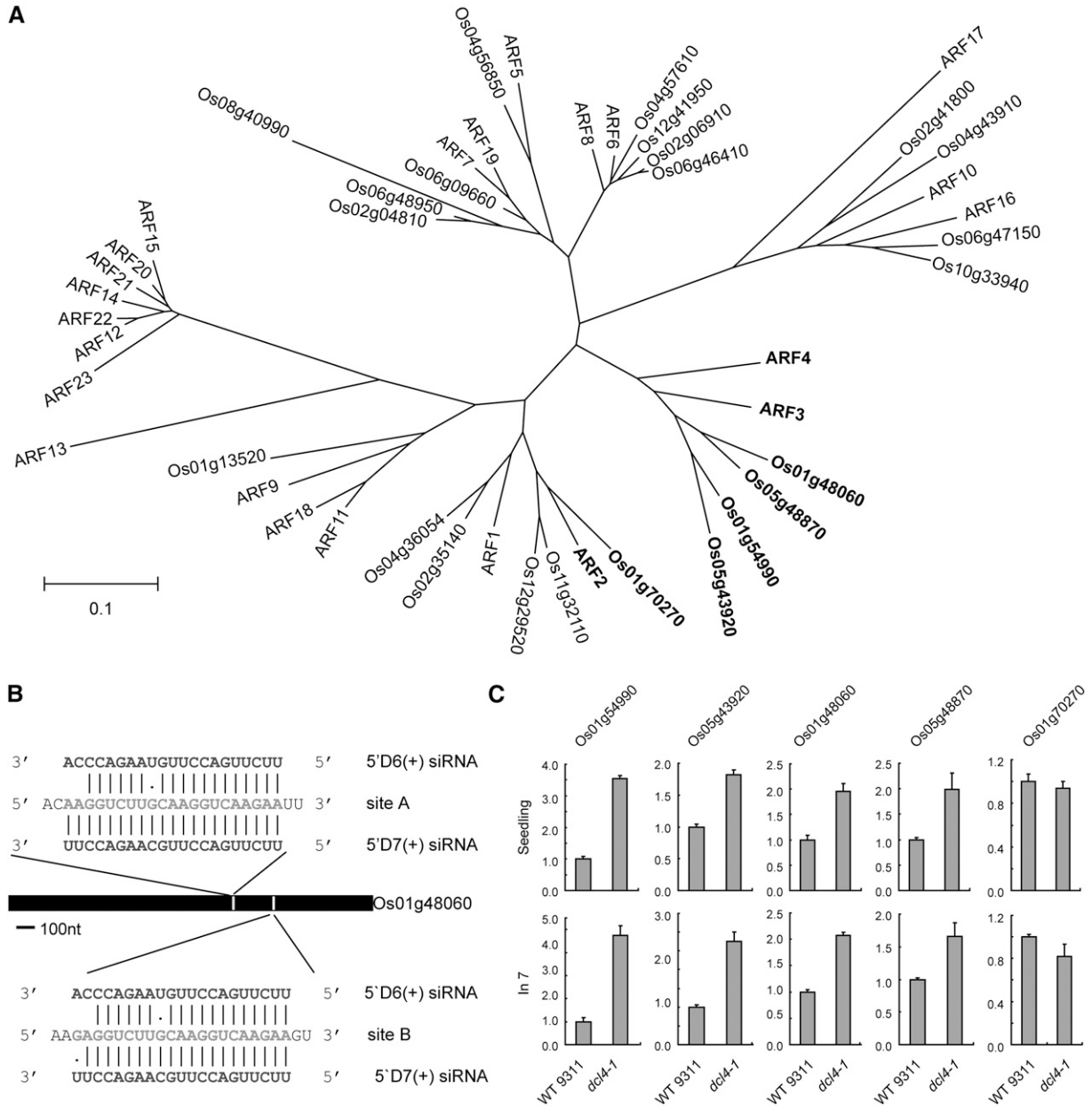

Figure 7. Target Genes of Os *TAS3* ta-siRNAs.

(A) Phylogenetic relationships of ARF proteins in *Arabidopsis* and rice. The predicted targets of *TAS3* ta-siRNAs are indicated in boldface. Bootstrap values (1000 replicates) for this tree are shown in Supplemental Figure 3 online. The bar indicates substitutions per site.

(B) The diagram represents a detailed example of Os *TAS3* ta-siRNAs and their target gene Os *01g48060*.

(C) Quantitative RT-PCR analysis of the expression of the five putative target genes of Os *TAS3* ta-siRNAs in wild-type 9311 rice and *dcl4-1*. The expression levels of the assayed genes were normalized according to the expression value of Os *EF-1*α, and the expression from wild-type 9311 was set to 1.0. Error bars indicate SD. Seedling, the aerial part of plants at 6 DAG; In7, inflorescence in the floral organ differentiation stage. Os *01g54990*, Os *05g43920*, Os *01g48060*, Os *05g48870*, and Os *01g70270* were previously named *ARF3*-likeB, *ARF3*-likeA, *ARF3*-like2, *ARF3*-like1, and *ARF2*-like, respectively (Williams et al., 2005).

a completely abaxialized epidermis (Timmermans et al., 1998; Juarez et al., 2004; Nogueira et al., 2007). The comparison of obvious phenotypes of *dcl4* in rice and *lbl1* in maize with their *Arabidopsis* counterpart reinforces the idea that polarity pathways vary in their importance in different plant species (Kidner and Timmermans, 2007). Although we do not know whether the rice *AS1* homolog (Os *AS1*) acts in proximal/distal patterning, like *ROUGH SHEATH2* in maize, or in adaxial/abaxial patterning, like *AS1* in *Arabidopsis*, from the distinct phenotypes of Os *dcl4* and At *dcl4*, we would predict that the ta-siRNA pathway may not be

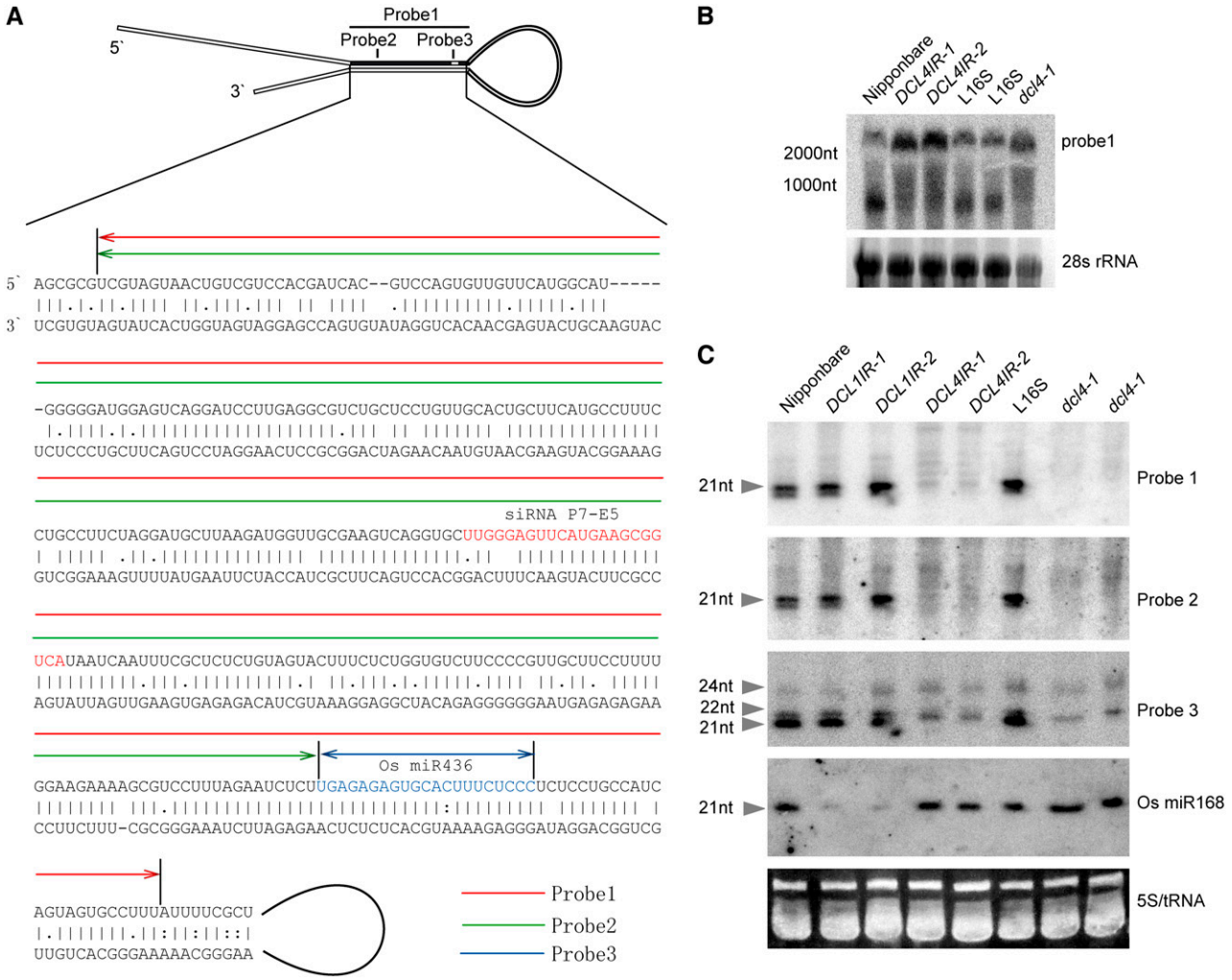

Figure 8. Expression Pattern of *AK120922* Transcript and Its Derived siRNAs in Different Mutants.

(A) Diagrammatic representation of the fold-back structure of *AK120922* RNA and the sequence alignment of the fold-back double-stranded sequences. Probes used in the RNA gel blot hybridization are underlined in different colors: red for probe 1, green for probe 2, and blue for probe 3. Probe 1 covers probe 2 and probe 3. Probe 3 represents the region previously identified as miR436. The previously identified siRNA P7-E5 is located within probe 2 and labeled in red.

(B) RNA gel blot analysis of the expression levels of *AK120922* in *DCL4IR* transformants and *dcl4-1* using probe 1. nt, nucleotides.

(C) *AK120922*-related siRNAs in *DCL1IR* transformants, *DCL4IR* transformants, and *dcl4-1*. Probe 1 and probe 2 were ^{32}P-labeled transcripts, and probe 3 was a specific LNA nucleotide probe.

directly coupled with Os *AS1* to redundantly regulate lateral organ polarity. Therefore, loss of function of Os DCL4, the major component ta-siRNA pathway, leads to severe developmental defects in rice.

TAS3 ta-siRNA, *ARF3/4-LIKE* Genes, and Lateral Organ Polarity

*ARF*s such as the ta-siRNA targets that are negatively regulated by *TAS3* ta-siRNAs play a role in lateral organ polarity determination in *Arabidopsis* (Pekker et al., 2005). Overexpression of a modified *ETT* cDNA in which *TAS3* ta-siRNA target sites were mutated (*35S:ETTAB*) produced a higher frequency of aberrant phenotypes than did overexpression of a wild-type *ETT* cDNA (*35S:ETT*), indicating that a higher ectopic expression level of the *TAS3* ta-siRNA target correlates with the severity of the abnormal phenotypes (Hunter et al., 2006). In maize, four *ARF3/ARF4*-like target genes of *TAS3* ta-siRNA have also been identified, although only *ARF3a* has been experimentally validated to be a target (Nogueira et al., 2007). Phylogenetic analysis reveals that *ARF3/ARF4*-like genes have been duplicated, resulting in four Os *ARF* genes highly related to *ARF3/ARF4* in rice (Williams et al., 2005). In this work, we demonstrate that all four Os *ARF* genes are also upregulated in rice *dcl4*, similar to the regulation of their homologs in *Arabidopsis*, whereas the distinct phenotypes of

dcl4 mutants hint that the functional divergence of *ARFs* and/or variation in their downstream genes would be another possible explanation for the abnormal defects in Os *dcl4*.

Relationship between Endogenous siRNAs Derived from Inverted Repeats and miRNAs in Plants

In this study, we identified an endogenous RNA, *AK120922*, that was upregulated in loss-of-function rice *dcl4* mutants. The *AK120922* transcript can form an inverted repeat structure similar to miRNA precursors. It has been proposed that miRNA genes evolved from the inverted duplication of target genes (Allen et al., 2004). During evolution, the duplicated genes would evolve from the original inverted repeat with a perfect match to transitional genes (containing a long fold-back structure with very few mismatches) and miRNA genes (Allen et al., 2004). Recently, this hypothesis was experimentally validated in *Arabidopsis* (Rajagopalan et al., 2006; Fahlgren et al., 2007). In rice, *AK120922* contains all of the features of transitional genes, and the 21-nucleotide siRNAs generated from the double-stranded region of *AK120922* are dependent on Os DCL4 but not Os DCL1. This discovery supports the existence of a third class of small RNAs either transitional between siRNA and miRNA or a novel miRNA that depends on DCL4.

Unlike miRNA genes, these loci with long inverted repeats are not conserved in plants (Lu et al., 2006). The lack of conservation at the sequence level and the diversity of these loci in plants may partially explain why loss of function of DCL4 in *Arabidopsis* and rice resulted in distinct phenotypes.

METHODS

Plant Materials

Rice (*Oryza sativa*) subsp *japonica* (Nipponbare) and *indica* (L16S, 9311) plants were used in this study. The *DCL4IR* and *DCL1IR* transformants were in the Nipponbare background (Liu et al., 2005). Nipponbare was used as the wild-type control of *DCL4IR* and *DCL1IR* transformants. The *dcl4-1* mutant was identified from an *indica* variety, L16S, and introgressed into 9311 by backcross. 9311 was used as the wild-type control of *dcl4-1*. The molecular markers used to PCR genotype the *dcl4-1* mutation were as follows: P1 (CX1240, 5′-CAGACGGTGTATGTAACACC-3′) and P2 (CX1794, 5′-CGGACTCCAAGACGCAATATGT-3′) for the wild type, with a predicted size of 637 bp; and P1 and P3 (CX1335, 5′-TTGCGATCACCACAGCTTGC-3′) for *dcl4-1* and the wild-type, with predicted sizes of 1.6 and 3 kb, respectively (Figure 2D). To map the *dcl4-1* mutant, every 10 plants with mutant phenotypes were pooled, and 66 pools were obtained from 660 F2 populations. Genomic DNA was extracted from each pool as a template for PCR-based genotyping.

Tissue Collection

Young inflorescences enclosed in sheaths were collected from plants grown in the field, frozen in liquid nitrogen immediately after harvest, and preserved in a −80°C refrigerator for RT-PCR, RNA gel blot analysis, and microarray hybridization. For biochemical analysis, inflorescences of ~4 cm in length were collected from the field. Callus tissues were induced from embryogenic calli on Murashige and Skoog medium with 2 mg/L 2,4-D for 30 d before harvesting. Seedlings were grown on Murashige and Skoog medium with a daylength of 16 h and a night of 8 h at 25°C.

Histological Analysis

The coleoptiles and first leaves of 3.5-DAG seedlings were fixed overnight with 2% glutaraldehyde and 1% paraformaldehyde. Tissues were dehydrated in a graded ethanol series, then transferred to propylene oxide and embedded in Spurr's resin (SPI-CHEM). Microtome sections at 3 μm were stained with 0.5% toluidine blue and observed with a light microscope (Olympus BX51 plus DP70).

Rice Oligonucleotide Array

The rice 70-mer oligonucleotide microarray was used in this study as described previously (Jiao et al., 2005; Ma et al., 2005).

RNA Isolation, Probe Labeling, and Microarray Hybridization

Rice inflorescences (~4 to 8 cm in length) were frozen in liquid nitrogen, and total RNA was isolated using RNAwiz reagent (Ambion) and purified with the RNeasy kit (Qiagen). For each sample, 100 μg of total RNA was labeled with aminoallyl-dUTP (Sigma-Aldrich) by reverse transcription. The aminoallyl-dUTP–labeled cDNAs were purified using a Microcon YM-30 filter (Millipore) and resuspended in 0.1 M $NaHCO_3$. The purified cDNAs were further fluorescently labeled by conjugating monofunctional Cy3 or Cy5 dye (Amersham) to the aminoallyl functional groups. Two independent biological replicates were performed with a dye swap. After coupling at room temperature for 1 h, the labeling reaction was stopped by ethanolamine. The labeled probes were separated from unincorporated dye using the QIAquick PCR purification kit (Qiagen) and concentrated with a Microcon YM-30 filter. The protocols for microarray hybridization, microarray slide washing, and array scanning were as described previously (Ma et al., 2005). Hybridized slides were scanned with a GenePix 4000B scanner (Axon), and independent TIFF images for Cy3 and Cy5 channels were used for subsequent analysis.

Microarray Data Processing

After manual removal of spots with aberrant morphology, microarray spot intensity signals were acquired using the Axon GenePix Pro 5.0 software package without correction for background, and each slide included two groups of intensity data corresponding to Cy5 and Cy3 channels. We first removed the dye effect on each slide using the LOWESS normalization method, which was applied to $\log_2$-transformed mutant versus wild-type expression values with two-sample hypothesis and equal variation assumptions. Subsequently, quartile normalization was applied to the LOWESS-normalized microarray data to remove biases among slides. For detection of differentially expressed spots between mutant and wild-type rice panicles, the normalized data were $\log_2$-transformed and fitted into a mixed-effect analysis of variance model with the software MAANOVA under an R environment. After multiple testing between pair-wise comparisons, spots with false discovery rate–corrected $P < 0.05$ were regarded as differentially expressed genes.

dsRNA Synthesis

A 568-bp PCR fragment was produced from the *GUS* gene using the sense primer CX1415 (5′-GAAGATCTGGTATCAGCGCGAAGTCT-3′) and the antisense primer CX1416 (5′-CCGCTCGAGTTCATAGAGATAACC-3′). The PCR fragment was cloned into pGEM-T Easy vector (Promega) for in vitro transcription. Both sense and antisense RNA transcripts produced by T7 RNA polymerase were equally mixed and denatured at 100°C for 5 min and annealed at room temperature for 10 min. dsRNAs were purified from a 1% agarose gel to remove single-stranded RNAs.

Preparation of Protein Extract

The total protein extract was prepared as described previously (Qi et al., 2005), and the protein concentration was adjusted to 2 mg/mL with exaction buffer (20 mM Tris-HCl, pH 7.5, 4 mM $MgCl_2$, 5 mM DTT, and 1 tablet/10 mL protease inhibitor cocktail from Roche) for the Dicer activity assay.

Dicer Activity Analysis

dsRNA (1 ng) was added to 30 μL of protein extract and 8 μL of 5× Dicer buffer (0.5 M NaCl, 5 mM ATP, 1 mM GTP, 6 mM $MgCl_2$, 125 mM creatine phosphate, 150 μg/mL creatine kinase, and 2 units of RNasin RNase inhibitor from Promega) in a total volume of 40 μL (Qi et al., 2005). The mixture was incubated at 30°C for 2 h. The reaction was stopped by adding Trizol solution and precipitated with 4 volumes of ethanol. The precipitate was resolved on a 15% denaturing PAGE gel and transferred to a Bio-Rad Zeta-Probe GT nylon membrane for RNA gel blot analysis. The produced siRNAs were detected with ^{32}P-labeled RNA probe.

Phylogenetic Analysis

Full-length protein sequences were used for phylogenetic analyses. The sequences derived from 29 known or predicted Os *ARF* genes were found in The Institute for Genomic Research rice genome annotation database (http://www.tigr.org/tdb/e2k1/osa1/GeneNameSearch.shtml) using "auxin response factor" as the search query. The 23 highly related Os ARF protein sequences were used for alignments. The protein sequences of 23 *ARF* genes from ARF1 to ARF23 were downloaded from The Arabidopsis Information Resource database (http://www.Arabidopsis.org/index.jsp), referring to the locus numbers as listed previously (Remington et al., 2004). Alignments of protein sequences were performed using ClustalX version 1.81 with default parameters (gap opening, 10.00; gap extension, 0.20; delay divergent sequences, 30%; DNA transition weight, 0.50) (see Supplemental Figure 5 online). A bootstrapping phylogenetic tree was constructed by the MEGA2 program with the Unweighted Pair Group Method and the Arithmetic Mean method. The number of bootstrap replicates was 1000.

RT-PCR and Real-Time PCR Analysis of Gene Expression

RT-PCR was performed as described previously to detect the expression of Os *DCL4* (Liu et al., 2005) using primer pairs CX0758 (5′-GGACTAGTTACACGAACGTCCTCTTCTTTTGGTAGGT-3′) and CX0857 (5′-CGATGAGAGAACTTCGAGAGCT-3′). The Os *EF-1*α gene was used as an internal loading control with the following primer pairs: CX1597 (5′-GCACGCTCTTCTTGCTTTCACTCT-3′) and CX1598 (5′-AAAGGTCACCACCATACCAGGCTT-3′).

Real-time PCR analysis was performed to measure transcript levels using the system reported previously (Deng et al., 2007). PCR was performed using hot-start Taq DNA polymerase (TaKaRa Taq Hot Start version; Code DR007B). For each sample, quantifications were made in triplicate. Melt curves were read at the end of each amplification by steps of 0.3°C from 65 to 95°C to ensure that the quantifications were derived from real PCR products and not primer dimers. Specific gene expression was normalized to the internal control gene Os *EF-1*α using the primers just described; the gene expression value of the wild type was used as a control and set at 1.0. For each target gene, primer pairs were as follows: for Os 05g48870, CX1548 (5′-GTGATACAGACCCTATGTGGCAT-3′) and CX1549 (5′-TTACTCGCATCGCTGGAGCAACT-3′); for Os 01g48060, CX1540 (5′-TTGGAAGCAGAGAGGCAGATCCAA-3′) and CX1541 (5′-AGGAAAACCCAGGGTTTCCACTT-3′); for Os 01g54990, CX2259 (5′-AAAGGCTTCAACACCTGGGA-3′) and CX2260 (5′-GGCTCATAACTAGGTCTAGA-3′); for Os 05g43920, CX2261 (5′-TGAAGAGCCTGAACCATCCA-3′) and CX2262 (5′-TTGGTTCGCTTAGACCCAGA-3′); and for Os 01g70270, CX2263 (5′-TCGATGGTGAATTGGTGTCT-3′) and CX2264 (5′-AGACTCCATGCGATCTACCT-3′).

RNA Gel Blot Analysis

Total RNAs were extracted using Trizol solution from the young panicles of rice and dissolved in RNase-free water. Small RNAs were enriched by adding the same volume of 8 M LiCl and centrifuging at 12,000 rpm for 30 min at 4°C. RNA filter hybridizations were performed as described previously (Liu et al., 2005). The templates for transcript probes 1 and 2 were amplified from rice genomic DNA by PCR with the following primers: for probe 1, CX0761 (5′-TCGTAGTAACTGTCGTCCACGA-3′) and CX0762 (5′-AAAGGCACTACTGATGGCAGGA-3′); for probe 2, CX0761 (5′-TCGTAGTAACTGTCGTCCACGA-3′) and CX1443 (5′-AGAGATTCTAAAGGACGCT-3′). The PCR products were then cloned into T-Easy vector under the control of the T7 promoter, and the templates for transcription of the RNA probes were linearized by PCR with the following primers: for probe 1, M13 (5′-GTAAAACGACGGCCAG-3′) and CX0762; for probe 2, M13 and CX1443. Probe 3 was end-labeled with LNA (5′-GGAGAAAGTGcAcTCTcTCA-3′; lowercase letters represent LNAs) (TaKaRa) (Valoczi et al., 2004). Probe for Os *TAS3* ta-siRNA was end-labeled with LNA (5′-GTGGGTCTTACAaGgTcAaGAA-3′; lowercase letters represent LNAs). To prepare RNA probe for *PSIR*, the template was amplified from the RNAi vector using primer CX1947 (5′-CCCTCCCAGGAAAAGTTCA-3′) and primer CX1948 (5′-CCAAGTTCAGGGATATGAGCA-3′). *DCL4IR* probe was prepared as described previously (Liu et al., 2005). End-labeled oligo DNA probe (5′-GTCCCGATCTGCACCAAGCGA-3′) was used to detect Os miR168.

Accession Number

The cDNA sequence for Os *DCL4* was deposited in the GenBank data library under accession number EU009924.

Supplemental Data

The following materials are available in the online version of this article.

Supplemental Figure 1. Mature Plants of *dcl4-1*.

Supplemental Figure 2. Accumulation of Os miRNAs as Revealed by RNA Filter Hybridization with End-Labeled Oligo DNA Probes.

Supplemental Figure 3. Neighbor-Joining Phylogenetic Tree of Protein Sequences with Bootstrap Values.

Supplemental Figure 4. Seventeen-Nucleotide Small RNA Massively Parallel Signature Sequencing Signatures Generated from the Fold-Back Region of *AK120922* Transcript.

Supplemental Figure 5. Multiple alignments of the ARF Protein Sequences by ClustalX.

Supplemental Table 1. Expression Data for Genes That Were Significantly Changed between the Inflorescences of Wild-Type and *DCL4IR* Transgenic Rice.

ACKNOWLEDGMENTS

We thank Catherine Kidner from the Royal Botanic Garden Edinburgh and the University of Edinburgh for helpful comments and English editing of the manuscript. We also thank Yonghong Wang from Jiayang Li's laboratory, Xia Wang, and Ying Lan for assistance with microscopy for morphologic analysis. We thank Lihuang Zhu for providing the *dcl4-1* allele. This work was supported by the National Natural Science Foundation of China (Grants 30621001 and 30325015 to X.C.), the State

High-Tech Project (Grant 2006AA10A101 to Y.X.), the National Basic Research Program of China (Grants 2005CB120806 and 2005CB522400), and the Chinese Academy of Sciences (Grant CXTD-S2005-2 to X.C.). The authors gratefully acknowledge the support of the K.C. Wong Education Foundation, Hong Kong.

Received April 12, 2007; revised September 2, 2007; accepted September 11, 2007; published September 28, 2007.

REFERENCES

Adenot, X., Elmayan, T., Lauressergues, D., Boutet, S., Bouche, N., Gasciolli, V., and Vaucheret, H. (2006). DRB4-dependent TAS3 trans-acting siRNAs control leaf morphology through AGO7. Curr. Biol. **16:** 927–932.

Allen, E., Xie, Z., Gustafson, A.M., and Carrington, J.C. (2005). MicroRNA-directed phasing during trans-acting siRNA biogenesis in plants. Cell **121:** 207–221.

Allen, E., Xie, Z., Gustafson, A.M., Sung, G.H., Spatafora, J.W., and Carrington, J.C. (2004). Evolution of microRNA genes by inverted duplication of target gene sequences in *Arabidopsis thaliana.* Nat. Genet. **36:** 1282–1290.

Asai, K., Satoh, N., Sasaki, H., Satoh, H., and Nagato, Y. (2002). A rice heterochronic mutant, mori1, is defective in the juvenile-adult phase change. Development **129:** 265–273.

Axtell, M.J., Jan, C., Rajagopalan, R., and Bartel, D.P. (2006). A two-hit trigger for siRNA biogenesis in plants. Cell **127:** 565–577.

Bartel, D.P. (2004). MicroRNAs: Genomics, biogenesis, mechanism, and function. Cell **116:** 281–297.

Borsani, O., Zhu, J., Verslues, P.E., Sunkar, R., and Zhu, J.K. (2005). Endogenous siRNAs derived from a pair of natural cis-antisense transcripts regulate salt tolerance in Arabidopsis. Cell **123:** 1279–1291.

Bouche, N., Lauressergues, D., Gasciolli, V., and Vaucheret, H. (2006). An antagonistic function for Arabidopsis DCL2 in development and a new function for DCL4 in generating viral siRNAs. EMBO J. **25:** 3347–3356.

Deng, W., Liu, C., Pei, Y., Deng, X., Niu, L., and Cao, X. (2007). Involvement of the histone acetyltransferase AtHAC1 in the regulation of flowering time via repression of FLOWERING LOCUS C in Arabidopsis. Plant Physiol. **143:** 1660–1668.

Dudley, N.R., Labbe, J.C., and Goldstein, B. (2002). Using RNA interference to identify genes required for RNA interference. Proc. Natl. Acad. Sci. USA **99:** 4191–4196.

Elbashir, S.M., Lendeckel, W., and Tuschl, T. (2001). RNA interference is mediated by 21- and 22-nucleotide RNAs. Genes Dev. **15:** 188–200.

Eshed, Y., Baum, S.F., Perea, J.V., and Bowman, J.L. (2001). Establishment of polarity in lateral organs of plants. Curr. Biol. **11:** 1251–1260.

Fahlgren, N., Howell, M.D., Kasschau, K.D., Chapman, E.J., Sullivan, C.M., Cumbie, J.S., Givan, S.A., Law, T.F., Grant, S.R., Dangl, J.L., and Carrington, J.C. (2007). High-throughput sequencing of Arabidopsis microRNAs: Evidence for frequent birth and death of MIRNA genes. PLoS ONE. **2:** e219.

Fahlgren, N., Montgomery, T.A., Howell, M.D., Allen, E., Dvorak, S.K., Alexander, A.L., and Carrington, J.C. (2006). Regulation of AUXIN RESPONSE FACTOR3 by TAS3 ta-siRNA affects developmental timing and patterning in Arabidopsis. Curr. Biol. **16:** 939–944.

Ferrario, S., Immink, R.G., and Angenent, G.C. (2004). Conservation and diversity in flower land. Curr. Opin. Plant Biol. **7:** 84–91.

Garcia, D., Collier, S.A., Byrne, M.E., and Martienssen, R.A. (2006). Specification of leaf polarity in Arabidopsis via the trans-acting siRNA pathway. Curr. Biol. **16:** 933–938.

Gasciolli, V., Mallory, A.C., Bartel, D.P., and Vaucheret, H. (2005). Partially redundant functions of Arabidopsis DICER-like enzymes and a role for DCL4 in producing trans-acting siRNAs. Curr. Biol. **15:** 1494–1500.

Henderson, I.R., Zhang, X., Lu, C., Johnson, L., Meyers, B.C., Green, P.J., and Jacobsen, S.E. (2006). Dissecting *Arabidopsis thaliana* DICER function in small RNA processing, gene silencing and DNA methylation patterning. Nat. Genet. **38:** 721–725.

Howell, M.D., Fahlgren, N., Chapman, E.J., Cumbie, J.S., Sullivan, C.M., Givan, S.A., Kasschau, K.D., and Carrington, J.C. (2007). Genome-wide analysis of the RNA-DEPENDENT RNA POLYMERASE6/DICER-LIKE4 pathway in Arabidopsis reveals dependency on miRNA- and tasiRNA-directed targeting. Plant Cell **19:** 926–942.

Hunter, C., Willmann, M.R., Wu, G., Yoshikawa, M., de la Luz Gutierrez-Nava, M., and Poethig, S.R. (2006). Trans-acting siRNA-mediated repression of ETTIN and ARF4 regulates heteroblasty in Arabidopsis. Development **133:** 2973–2981.

Itoh, J., Nonomura, K., Ikeda, K., Yamaki, S., Inukai, Y., Yamagishi, H., Kitano, H., and Nagato, Y. (2005). Rice plant development: From zygote to spikelet. Plant Cell Physiol. **46:** 23–47.

Jiao, Y., et al. (2005). A tiling microarray expression analysis of rice chromosome 4 suggests a chromosome-level regulation of transcription. Plant Cell **17:** 1641–1657.

Jones-Rhoades, M.W., Bartel, D.P., and Bartel, B. (2006). MicroRNAs and their regulatory roles in plants. Annu. Rev. Plant Biol. **57:** 19–53.

Juarez, M.T., Twigg, R.W., and Timmermans, M.C. (2004). Specification of adaxial cell fate during maize leaf development. Development **131:** 4533–4544.

Kerstetter, R.A., Bollman, K., Taylor, R.A., Bomblies, K., and Poethig, R.S. (2001). KANADI regulates organ polarity in Arabidopsis. Nature **411:** 706–709.

Kidner, C.A., and Martienssen, R.A. (2005). The developmental role of microRNA in plants. Curr. Opin. Plant Biol. **8:** 38–44.

Kidner, C.A., and Timmermans, M.C. (2007). Mixing and matching pathways in leaf polarity. Curr. Opin. Plant Biol. **10:** 13–20.

Kikuchi, S., et al. (2003). Collection, mapping, and annotation of over 28,000 cDNA clones from japonica rice. Science **301:** 376–379.

Kim, J.K., Gabel, H.W., Kamath, R.S., Tewari, M., Pasquinelli, A., Rual, J.F., Kennedy, S., Dybbs, M., Bertin, N., Kaplan, J.M., Vidal, M., and Ruvkun, G. (2005). Functional genomic analysis of RNA interference in *C. elegans.* Science **308:** 1164–1167.

Kurihara, Y., and Watanabe, Y. (2004). Arabidopsis micro-RNA biogenesis through Dicer-like 1 protein functions. Proc. Natl. Acad. Sci. USA **101:** 12753–12758.

Lagos-Quintana, M., Rauhut, R., Lendeckel, W., and Tuschl, T. (2001). Identification of novel genes coding for small expressed RNAs. Science **294:** 853–858.

Lau, N.C., Lim, L.P., Weinstein, E.G., and Bartel, D.P. (2001). An abundant class of tiny RNAs with probable regulatory roles in *Caenorhabditis elegans.* Science **294:** 858–862.

Lee, R.C., and Ambros, V. (2001). An extensive class of small RNAs in *Caenorhabditis elegans.* Science **294:** 862–864.

Liu, B., Li, P., Li, X., Liu, C., Cao, S., Chu, C., and Cao, X. (2005). Loss of function of OsDCL1 affects microRNA accumulation and causes developmental defects in rice. Plant Physiol. **139:** 296–305.

Lu, C., Kulkarni, K., Souret, F.F., MuthuValliappan, R., Tej, S.S., Poethig, R.S., Henderson, I.R., Jacobsen, S.E., Wang, W., Green, P.J., and Meyers, B.C. (2006). MicroRNAs and other small RNAs enriched in the Arabidopsis RNA-dependent RNA polymerase-2 mutant. Genome Res. **16:** 1276–1288.

Ma, L., et al. (2005). A microarray analysis of the rice transcriptome and its comparison to Arabidopsis. Genome Res. **15:** 1274–1283.

Margis, R., Fusaro, A.F., Smith, N.A., Curtin, S.J., Watson, J.M., Finnegan, E.J., and Waterhouse, P.M. (2006). The evolution and diversification of Dicers in plants. FEBS Lett. **580:** 2442–2450.

Mette, M.F., Aufsatz, W., van der Winden, J., Matzke, M.A., and Matzke, A.J. (2000). Transcriptional silencing and promoter methylation triggered by double-stranded RNA. EMBO J. **19:** 5194–5201.

Nagasaki, H., Itoh, J., Hayashi, K., Hibara, K., Satoh-Nagasawa, N., Nosaka, M., Mukouhata, M., Ashikari, M., Kitano, H., Matsuoka, M., Nagato, Y., and Sato, Y. (2007). The small interfering RNA production pathway is required for shoot meristem initiation in rice. Proc. Natl. Acad. Sci. USA **104:** 14867–14871.

Nobuta, K., Venu, R.C., Lu, C., Belo, A., Vemaraju, K., Kulkarni, K., Wang, W., Pillay, M., Green, P.J., Wang, G.L., and Meyers, B.C. (2007). An expression atlas of rice mRNAs and small RNAs. Nat. Biotechnol. **25:** 473–477.

Nogueira, F.T., Madi, S., Chitwood, D.H., Juarez, M.T., and Timmermans, M.C. (2007). Two small regulatory RNAs establish opposing fates of a developmental axis. Genes Dev. **21:** 750–755.

Park, W., Li, J., Song, R., Messing, J., and Chen, X. (2002). CARPEL FACTORY, a Dicer homolog, and HEN1, a novel protein, act in microRNA metabolism in *Arabidopsis thaliana.* Curr. Biol. **12:** 1484–1495.

Pekker, I., Alvarez, J.P., and Eshed, Y. (2005). Auxin response factors mediate Arabidopsis organ asymmetry via modulation of KANADI activity. Plant Cell **17:** 2899–2910.

Prasad, K., Parameswaran, S., and Vijayraghavan, U. (2005). OsMADS1, a rice MADS-box factor, controls differentiation of specific cell types in the lemma and palea and is an early-acting regulator of inner floral organs. Plant J. **43:** 915–928.

Qi, Y., Denli, A.M., and Hannon, G.J. (2005). Biochemical specialization within Arabidopsis RNA silencing pathways. Mol. Cell **19:** 421–428.

Rajagopalan, R., Vaucheret, H., Trejo, J., and Bartel, D.P. (2006). A diverse and evolutionarily fluid set of microRNAs in *Arabidopsis thaliana.* Genes Dev. **20:** 3407–3425.

Reinhart, B.J., Weinstein, E.G., Rhoades, M.W., Bartel, B., and Bartel, D.P. (2002). MicroRNAs in plants. Genes Dev. **16:** 1616–1626.

Remington, D.L., Vision, T.J., Guilfoyle, T.J., and Reed, J.W. (2004). Contrasting modes of diversification in the Aux/IAA and ARF gene families. Plant Physiol. **135:** 1738–1752.

Schauer, S.E., Jacobsen, S.E., Meinke, D.W., and Ray, A. (2002). DICER-LIKE1: Blind men and elephants in Arabidopsis development. Trends Plant Sci. **7:** 487–491.

Schmidt, R.J., and Ambrose, B.A. (1998). The blooming of grass flower development. Curr. Opin. Plant Biol. **1:** 60–67.

Sunkar, R., Girke, T., Jain, P.K., and Zhu, J.K. (2005a). Cloning and characterization of microRNAs from rice. Plant Cell **17:** 1397–1411.

Sunkar, R., Girke, T., and Zhu, J.K. (2005b). Identification and characterization of endogenous small interfering RNAs from rice. Nucleic Acids Res. **33:** 4443–4454.

Tang, G., Reinhart, B.J., Bartel, D.P., and Zamore, P.D. (2003). A biochemical framework for RNA silencing in plants. Genes Dev. **17:** 49–63.

Timmermans, M.C., Schultes, N.P., Jankovsky, J.P., and Nelson, T. (1998). Leafbladeless1 is required for dorsoventrality of lateral organs in maize. Development **125:** 2813–2823.

Valoczi, A., Hornyik, C., Varga, N., Burgyan, J., Kauppinen, S., and Havelda, Z. (2004). Sensitive and specific detection of microRNAs by northern blot analysis using LNA-modified oligonucleotide probes. Nucleic Acids Res. **32:** e175.

Vaucheret, H. (2006). Post-transcriptional small RNA pathways in plants: Mechanisms and regulations. Genes Dev. **20:** 759–771.

Vazquez, F., Vaucheret, H., Rajagopalan, R., Lepers, C., Gasciolli, V., Mallory, A.C., Hilbert, J.L., Bartel, D.P., and Crete, P. (2004). Endogenous trans-acting siRNAs regulate the accumulation of Arabidopsis mRNAs. Mol. Cell **16:** 69–79.

Williams, L., Carles, C.C., Osmont, K.S., and Fletcher, J.C. (2005). A database analysis method identifies an endogenous trans-acting short-interfering RNA that targets the Arabidopsis ARF2, ARF3, and ARF4 genes. Proc. Natl. Acad. Sci. USA **102:** 9703–9708.

Xie, Z., Allen, E., Wilken, A., and Carrington, J.C. (2005). DICER-LIKE 4 functions in trans-acting small interfering RNA biogenesis and vegetative phase change in *Arabidopsis thaliana.* Proc. Natl. Acad. Sci. USA **102:** 12984–12989.

Xie, Z., Johansen, L.K., Gustafson, A.M., Kasschau, K.D., Lellis, A.D., Zilberman, D., Jacobsen, S.E., and Carrington, J.C. (2004). Genetic and functional diversification of small RNA pathways in plants. PLoS Biol. **2:** E104.

Yoshikawa, M., Peragine, A., Park, M.Y., and Poethig, R.S. (2005). A pathway for the biogenesis of trans-acting siRNAs in Arabidopsis. Genes Dev. **19:** 2164–2175.

Zamore, P.D., Tuschl, T., Sharp, P.A., and Bartel, D.P. (2000). RNAi: double-stranded RNA directs the ATP-dependent cleavage of mRNA at 21 to 23 nucleotide intervals. Cell **101:** 25–33.